MATHEMATICAL REPRESENTATION OF A CFD MODEL FOR ARTIFICIAL FOG SPRAY INVESTIGATION

M.Sc. Todorov P. [1]
"G. Nadjakov" Institute of Solid State Physics, Bulgarian Academy of Sciences [1]
pv_todorov@abv.bg

Abstract: *We present and explain the mathematical apparatus used in a numerical simulation model created with ANSYS CFX Software. The purpose of the model is to perform computations of fog parameters in different points of artificially generated fog sprays, which are then used to calibrate a novel type of fog sensors. By changing the distance between the nozzle and the measuring laser beam of the sensor, we can assess how the number flow rate and diameter distribution of fog droplets are varied within in the spray. This work is related to improving European security by introducing systems for quick counteraction to terrorist attacks, industrial accidents and natural disasters. These systems use artificial fog generation to collect and deposit on the ground harmful aerosols dispersed in air, especially CBRN agents. Our newly developed fog sensors operate on the basis of the electromagnetic echo effect to control the decontamination process. In order to optimize the work of the sensors, it is crucial to investigate fogs and their ability to absorb harmful substances from air. The most important fog parameters that influence the efficiency of the cleaning process are the number of droplets and their size.*

Keywords: COMPUTATIONAL FLUID DYNAMICS, ELECTROMAGNETIC ECHO EFFECT, FOG SENSOR, LASER IRRADIATION

1. Introduction

The investigations of our team are related to interactions between electromagnetic field and matter. We study a phenomenon consequent to these interactions – the *surface photo-charge effect (SPCE)*, and develop sensors, which operate on its basis. In 2019, O. Ivanov, who observed the effect for the first time, suggested that the name of the effect is changed to *electromagnetic echo effect (EMEE)*, since it better describes its nature. In addition, in this way it will not be confused with the *photoelectric effect* [1]. The *EMEE* is observed during interaction of any solid with an electromagnetic field, which induces an electric, alternating potential difference with the same frequency as the frequency of the incident wave. The induced electrical signal exists between the irradiated solid and the common electrical ground of the system. It can be measured via an electrode, which either can be either in contact with the irradiated solid body, or can be placed in near proximity. This means that the measurement can be made in a contactless way and also quite fast [2]. The principle scheme of measurement is shown in *Fig. 1*.

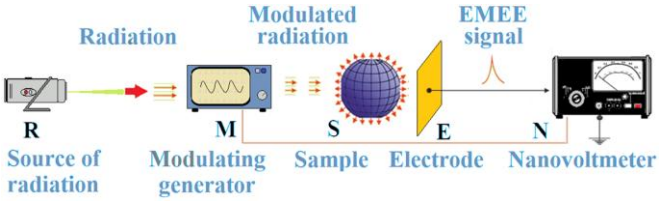

Fig. 1. *General scheme for EMEE observation: (R) electromagnetic radiation source, (M) radiation modulator, (S) irradiated solid sample, (E) signal measuring electrode, (N) signal measuring device – nanovoltmeter.*

An important feature of the *EMEE* is that each solid responds to the irradiation of the electromagnetic field with a specific signal, which is influenced by the inherent properties of the material. The *EMEE* has been registered with modulation frequencies between *1 Hz* and *1 GHz*, and has been observed in a wide range of the electromagnetic spectrum – from the infrared, throughout the visible and up to the beginning of the ultraviolet spectrum [3]. We suppose that it is present within the whole electromagnetic spectrum. The measured value of *EMEE* can depend on many factors, such as *intensity of irradiation*, *wavelength*, *area of irradiated region*, *surface condition*, *surface structure*, *chemical composition*, *type of material*, etc. [4]. Any change in a solid (*conductivity*, *composition*, *mechanical defects*, etc.) leads to a change in the measured signal. This reveals the huge potential of the *EMEE* to be used for development of various types of sensors.

We have applied our experience with the *EMEE* to participate in the development of new types of fog sensors under a European project related to security with acronym *COUNTERFOG*. Its aim is to create systems for quick large-scale decontamination by releasing special fogs, in cases of terrorist attacks with *CBRN* agents, industrial accidents and disasters [5]. The tasks of our team are to control the fog generators. These include monitoring of various properties of fog – *density*, *diameter*, *number* and *speed* of droplets, *chemical composition*. Within this project, new types of fog sensors have been developed, which are able to control fog parameters over very large distances, and also to detect in real time the presence of dangerous substances in the composition of fog [6].

During the development of these sensors, it was necessary to study the absorption capabilities of fogs, and it was found that mainly the number and diameter of droplets influence the efficiency of the process of collection of harmful substances from air. This is why we created a numerical model to simulate artificially produced fog sprays, for the purpose of investigation of fog characteristics in different areas of the sprays. In this way, we can study fog parameters at specific points of the streams and calibrate our sensors, which use modulated laser beams to take the measurements. We did a research on the change in the number flow rate of droplets as a function of the distance from the nozzle. Calculations show that if we know some of the parameters of the nozzle, the distance at which the number of droplets is approximately the same for different nozzles, can be determined. Thus, if we were to move the measuring laser beam, ensuring that the number flow rate of droplets is identical, then the measured signal will be a function only of the diameter of the droplets. In this way, we can calibrate our sensors to measure the diameter of droplets, since only their size will influence the signal. The model can simulate the output flow of different nozzles and calculate the diameter distribution and the number flow rate through specific locations of the sprays [7]. In this work, we present the mathematical algorithms on which the model is based.

2. Prerequisites for Solving the Problem

Computational Fluid Dynamics

Computational Fluid Dynamics (*CFD*) is a branch of fluid mechanics that uses computer power to perform numerical analyses of fluids in movement and the forces that influence them. Nowadays, advanced software and hardware allow high-resolution interactive 3D models to be created and complex problems to be solved with unprecedented accuracy. Scientists and engineers in various fields use *CFD* to study the nature of fluid flow phenomena, the behaviour of systems involving fluid flow, heat and mass transfer, combustion, evaporation and other related physical processes, design machines and optimize processes. The fundamental basis of most *CFD* problems are theory equations, which are used to mathematically describe the physics of fluid flow. These are the continuity equation and the momentum equation, also known as the *Navier-Stokes* equations, are needed to describe the state of any type of flow (how the *velocity*, *pressure*, *temperature* and *density* are related) and are generally solved for all flows in *CFD* modelling. They are based on three conservation laws: *conservation of mass*, *momentum* and *energy*. These partial

differential equations were derived in the early 19th century and have no general analytical solution but can be discretized and solved numerically. There exist a number of solution methodologies used in *CFD* codes. The most common one is known as the *finite volume method (FVM)*. The technique includes division of the region of interest into small sub-volumes. The equations are discretized and solved iteratively for each of them. As a result, an approximation of the value of each variable at specific points throughout the investigated domain is obtained. In this way, a full picture of the behaviour of the flow is assembled. In this work, we present a model created based on this method using the free student version of the *ANSYS CFX* Software.

Modelling Approach

Multiphase flow involves the simultaneous presence of different phases in solid, liquid or vapour state of matter. Although multiphase flow involving three phases can also exist, most multiphase engineering applications are two-phase flow. Two-phase flow refers to the interactive flow of two distinct phases with common interfaces, with each phase representing a mass or volume of matter. The main categories of multiphase flows are *gas-liquid*, *gas-solid*, *liquid-solid* and *three-phase* flows. A *flow pattern* describes the geometrical distribution of the phases and depends on the geometry of the flow domain - *separated*, *mixed* or *dispersed*. In *dispersed flows*, one phase is widely distributed as solid particles or bubbles in another continuous phase. In order to describe and predict the complex physics of multiphase flows, numerical studies use various models to optimise time and computing resources. This has led to the development of models that can account for different levels of information and accuracy for specific applications.

In our model, a coupled solver is implemented and a *vertex based FVM* approach is used for discretisation of the transport equations. In a *coupled solver*, the momentum and continuity equations are solved simultaneously. That is why it requires more memory and time for calculations than segregated solvers. On the other hand, a coupled solver usually needs less iterations to achieve convergence. Two distinct multiphase flow models are available in *CFX* - an *Eulerian-Eulerian multiphase model* and a *Lagrangian Particle Tracking multiphase model*. We use the latter for simulating and tracking the flow of fog droplets ejected from the nozzles. *Particle transport modelling* is a type of multiphase model, where particles are tracked through the flow in a Lagrangian way, rather than being modelled as an extra Eulerian phase. The flow of particulate phase is modelled by tracking a small number of droplets from the injection point through the continuum fluid (air), until they escape the domain. The tracking is done by forming a set of ordinary differential equations in time for each droplet - for *position*, *velocity*, *temperature*, and *masses* of species. These equations are then integrated using a simple integration method to calculate the behaviour of the droplets as they traverse the flow domain.

3. Solution of the Examined Problem

Details and assumptions on the model

In our model, we study the hollow cone sprays with distinct diameter distributions of droplets produced by nozzles at a constant fluid pressure of *5 bar*. The *chemical composition* and *velocity* of droplets (depending on the *atomizing pressure* and their *mass*, respectively *size*) are kept the same. The sensor's laser beam is placed at a specific distance from each nozzle, which ensures relatively identical droplet flow rates. This reduces the number of variable parameters to one – the *droplet diameter distribution*, which is determined by the nozzle. Hence, we can study the signal dependence on the droplet diameter distribution and calibrate our devices.

The model is considered *stationary* – the process parameters do not change in time and the results define the equilibrium state of the process. As the input parameters (*water pressure*, *flow rate*, *environmental conditions*, *nozzle geometry*) are either constant or vary insignificantly, we conclude that the output parameters in a certain point of interest (*droplet flow rate*, *velocity*, *size distribution*) will also be invariant of time. The size distribution in different points varies slightly due to evaporation. The actual liquid atomization process is not modelled, even though the software package supports primary and secondary liquid breakup models, since this would only increase the computational load tremendously. Instead, the droplets are injected from an injection point with a predefined diameter distribution, given in the manufacturer's datasheet of the corresponding nozzle. The flow of droplets is fully axisymmetric around the axis, normal to the nozzle orifice. The nozzle is placed perpendicularly over the laser beam. The geometric model resembles a 30-degree slice of the volume of the spray (*Fig. 2a*), as we are only interested in the flow through the laser beam and in the area close to it. The nozzle orifice is located where the central axis crosses the top face. The laser beam only passes through half of the spray until it reaches the central axis. Therefore, the resulting droplet flow rate must be doubled, again assuming that the other half is identical to the investigated one.

In order to obtain a relatively identical size of the elements in the mesh and consistency of the results when simulating different distances from the nozzle, the height of each element is set to be *4 mm*. If the distance is not a multiple of four, one layer of elements (usually at the top or bottom) will have a different height. As the shape of the spray resembles a hollow cone and most of the droplets flow closer to the edge of the volume, the element width is biased towards this area, in order to increase the accuracy of the droplet trajectories (*Fig. 2b*).

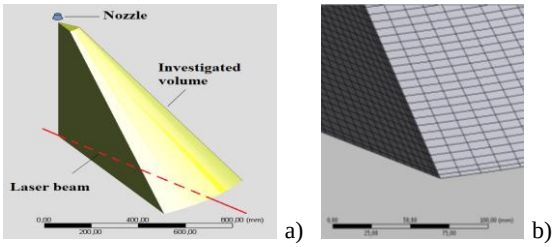

a) b)

Fig. 2. *Geometry of the investigated volume (a); the elemental mesh (b).*

Two phases are present in the domain description – *Air* and *Water*. *Water* is defined as a pure substance (H_2O in liquid state) in the material description, while *Air* is a mixture of the materials *Air Ideal Gas* and H_2O in gaseous state. The evaporation from water droplets is defined as a mass transfer of H_2O from *Water* to H_2O present in the *Air* mixture. The transfer rate is determined by the content of H_2O in *Air* and the heat transfer rate. The entire volume is occupied by *Air*, while *Water* is injected from the injection region in the form of polydispersed particles. The two phases are *fully coupled*, meaning that any change in the velocity field of one will affect the velocity field of the other. Additional forces taken into account are *drag*, *buoyancy* and *turbulent dispersion*.

The injection parameters are defined using the data given by the manufacturer. The *injection velocity* is derived from the nozzle orifice *diameter* and the *mass flow rate*. The injection angle is at *45°* from the central axis. The droplet diameter spectrum is defined using *minimum*, *maximum*, *mean diameters* and *standard deviation*. The droplet temperature is set to be *4° C*, which is the temperature of tap water. The number of trajectories, used to represent the flow was set to *100 000*. The domain has two boundaries – the laser beam face and all other faces. They have identical conditions – openings to the environment with zero relative pressure difference. The reason for defining them separately is to filter the droplet trajectories and isolate the ones, which flow only through the laser beam boundary. The *number flow rate* through the laser will be determined by these trajectories.

Mathematics of the model

***Governing equations*:** The set of transport equations solved by the software are the unsteady *Navier-Stokes* equations in their conservation form. They calculate the instantaneous mass, momentum and energy. *Eq. 1* is the continuity equation, *Eq. 2* is the momentum equation and *Eq. 4* is the total energy equation:

$$\frac{\partial \rho}{\partial t}+\nabla\cdot(\rho\,\boldsymbol{U})=0 \tag{1}$$

Where $\boldsymbol{\rho}$ is density and $\boldsymbol{U}$ is instantaneous velocity.

$$\frac{\partial(\rho\,\boldsymbol{U})}{\partial t}+\nabla\cdot(\rho\,\boldsymbol{U}\otimes\boldsymbol{U})=-\nabla p+\nabla\cdot\tau+\boldsymbol{S_M} \tag{2}$$

Here, $\boldsymbol{\rho}$ is density, $\boldsymbol{U}$ is instantaneous velocity, $\boldsymbol{S_M}$ is momentum source, and $\boldsymbol{\tau}$ is the stress tensor, which is related to strain rate by *Eq. 3*:

$$\tau=\mu\left(\nabla\boldsymbol{U}+(\nabla\boldsymbol{U})^{T}-\frac{2}{3}\delta\,\nabla\cdot\boldsymbol{U}\right) \tag{3}$$

Where $\boldsymbol{\mu}$ is molecular (dynamic) viscosity, $\boldsymbol{U}$ is instantaneous velocity, $\boldsymbol{T}$ is thermodynamic temperature and $\boldsymbol{\delta}$ is identity matrix or Kronecker Delta function.

$$\frac{\partial(\rho\,h_{\text{tot}})}{\partial t}-\frac{\partial p}{\partial t}+\nabla\cdot\left(\rho\,\boldsymbol{U}\,h_{\text{tot}}\right)= =\nabla\cdot(\lambda\,\nabla T)+\nabla\cdot(\boldsymbol{U}\cdot\tau)+\boldsymbol{U}\cdot\boldsymbol{S_M}+\boldsymbol{S_E} \tag{4}$$

Here, $\nabla\cdot(\boldsymbol{U}\cdot\tau)$ represents the work due to viscous forces, $\boldsymbol{U}\cdot\boldsymbol{S_M}$ represents the work due to external momentum sources (it is neglecetd), $\boldsymbol{S_M}$ is momentum source, $\boldsymbol{S_E}$ is energy source, and $\boldsymbol{h_{tot}}$ is the total enthalpy, which is related to the static enthalpy $\boldsymbol{h\,(T,\,p)}$ by *Eq. 5*:

$$h_{\text{tot}}=h+\frac{1}{2}\boldsymbol{U}^{2} \tag{5}$$

Just as the fluid affects the particles, there is a counteracting influence of the particles on the fluid. This effect is termed as *coupling* between phases. If the particles also affect the fluid behaviour, then the interaction is termed *two-way coupling*, which is our case. The forces acting on the particle traveling in a continuous fluid medium that affect the particle acceleration are due to the difference in velocity between the particle and fluid, as well as to the displacement of the fluid by the particle. The equation of motion for such a particle is given in *Eq. 6*:

$$m_P\frac{d\boldsymbol{U}_P}{dt}=\boldsymbol{F}_{\text{D}}+\boldsymbol{F}_{\text{B}}+\boldsymbol{F}_{\text{R}}+\boldsymbol{F}_{\text{VM}}+\boldsymbol{F}_P+\boldsymbol{F}_{\text{BA}} \tag{6}$$

Where $\boldsymbol{F_D}$ is drag force acting on the particle, $\boldsymbol{F_B}$ is buoyancy force due to gravity, $\boldsymbol{F_R}$ represents forces due to domain rotation (centripetal and Coriolis forces), $\boldsymbol{F_{VM}}$ is virtual (or added) mass force, $\boldsymbol{F_P}$ is pressure gradient force, $\boldsymbol{F_{BA}}$ is Basset force or history term which accounts for the deviation in flow pattern from a steady state. We chose to account only for drag and buoyancy forces.

***Drag force*:** A water droplet travelling through air has two significant forces acting upon it - a gravitational force acting vertically downward and an *aerodynamic drag force* acting opposite to the direction of motion. Assuming that air is stationary before starting droplet injection from the nozzle, the drag force $\boldsymbol{F_D}$ increases with increasing slip droplet velocity $\boldsymbol{U_S}$ (he relative velocity between the droplet and the air), and is directly related to the drag coefficient $\boldsymbol{C_D}$ (*Eq. 7*):

$$C_D=\frac{2F_D}{\rho U_S^2 A} \tag{7}$$

Here $\boldsymbol{\rho}$ is the density of air and $\boldsymbol{A}$ is the cross-sectional area perpendicular to the direction of motion. For spherical particles, $A = \pi r^2$ and the drag coefficient is set to 0.44.

***Buoyant force*:** The *buoyancy force* is the force on a particle immersed in a fluid. *Eq. 8* gives the buoyant force $\boldsymbol{F_B}$:

$$\boldsymbol{F}_{\text{B}}=\left(m_P-m_{\text{F}}\right)\boldsymbol{g}=\frac{\pi}{6}d_P^3\left(\rho_P-\rho_{\text{F}}\right)\boldsymbol{g} \tag{8}$$

Where $\boldsymbol{m_P}$ is the mass of the particle, $\boldsymbol{m_F}$ is the mass of the displaced fluid, $\boldsymbol{\rho_F}$ is density of the fluid, $\boldsymbol{\rho_P}$ is density of the particle, $\boldsymbol{d_P}$ is diameter of the particle, and $\boldsymbol{g}$ is the gravity vector. The buoyancy force has no contribution to the particle momentum source into the continuous phase.

***Heat transfer*:** Three physical processes govern the rate of change of temperature: *convective heat transfer*, *latent heat transfer* associated with *mass transfer*, and *radiative heat transfer*. *Eq. 9* gives the *convective heat transfer* $\boldsymbol{Q_C}$:

$$Q_C=\pi\,d\,\lambda\,\text{Nu}\left(T_G-T\right) \tag{9}$$

Where $\boldsymbol{\lambda}$ is the thermal conductivity of the fluid, $\boldsymbol{T_G}$ and $\boldsymbol{T}$ are the temperatures of the fluid and of the particle, respectively, and $\boldsymbol{Nu}$ is the *Nusselt number* given by *Eq. 10*:

$$\text{Nu}=2+0.6\,\text{Re}^{\frac{1}{2}}\left(\mu\,\frac{C_P}{\lambda}\right)^{\frac{1}{3}} \tag{10}$$

Here, $\boldsymbol{Re}$ is the Reynolds number, $\boldsymbol{C_P}$ is the specific heat, $\boldsymbol{\lambda}$ is the thermal conductivity, and $\boldsymbol{\mu}$ is the molecular (dynamic) viscosity of the fluid. *Latent heat transfer* associated with mass transfer $\boldsymbol{Q_M}$ is given by *Eq. 11*:

$$Q_M=\Sigma\frac{dm_C}{dt}\,V \tag{11}$$

Where the sum is taken over all components of the particle for which heat transfer is taking place. The latent heat of vaporization $\boldsymbol{V}$ is temperature dependent, and is obtained directly from the information in the database for the liquid in the particle and its vapor; $\boldsymbol{m_C}$ is the mass of the constituent in the particle. *Eq. 12* gives the *radiative heat transfer* $\boldsymbol{Q_R}$ for a particle:

$$Q_R=\varepsilon_p\,\pi\,d_p^{\,2}\left(\pi\,I-\sigma\,n^2\,T_p^{\,4}\right) \tag{12}$$

Where $\boldsymbol{d_p}$ is the diameter of the particle, $\boldsymbol{T_p}$ is its uniform temperature, $\boldsymbol{\varepsilon_p}$ is the particle's emissivity, $\boldsymbol{I}$ is the radiation intensity on the particle's surface at the location of the particle, $\boldsymbol{n}$ is the refractive index of the fluid, and $\boldsymbol{\sigma}$ is the Stefan-Boltzmann constant. An equivalent amount of heat can be removed from the radiation field. Therefore, the rate of change of temperature for the particle can be calculated using *Eq. 13*:

$$\Sigma\left(m_C\,C_P\right)\frac{dT}{dt}=Q_C+Q_M+Q_R \tag{13}$$

Here, the sum in this equation is taken over all components of the particle including those not affected by mass transfer.

***Liquid evaporation model*:** This is a model for particles with heat transfer and one component of mass transfer, in which the continuous gas phase is at a higher temperature than the particles. When the particle is below the boiling point, the mass transfer is given by *Eq. 14*:

$$\frac{dm_C}{dt}=\pi\,d_P\,\rho_F\,D_F\,\text{Sh}\,\frac{W_C}{W_G}\log\left(\frac{1-X^*}{1-X_G}\right) \tag{14}$$

Where $\boldsymbol{m_C}$ is the mass of the constituent in the particle, $\boldsymbol{\rho_F}$ $\boldsymbol{D_F}$ is the dynamic diffusivity of the mass fraction in the continuum, $\boldsymbol{W_C}$ and $\boldsymbol{W_G}$ are the molecular weights of the vapor and the mixture in the continuous phase, $\boldsymbol{X_G}$ is the molar fraction in the gas phase, and $\boldsymbol{X^*}$ is the equilibrium mole fraction at the droplet surface defined as $\boldsymbol{P_{vap}}$ divided by the pressure in the continuous phase, and $\boldsymbol{Sh}$ is the Sherwood number (*Eq. 15*):

$$\text{Sh}=2+0.6\,\text{Re}^{\frac{1}{2}}\left(\frac{\mu}{\rho D}\right)^{\frac{1}{3}} \tag{15}$$

$\boldsymbol{Re}$ is Reynolds number, $\boldsymbol{\rho}$ is the density, $\boldsymbol{\mu}$ is the molecular (dynamic) viscosity of the fluid, $\boldsymbol{D}$ is the mass diffusivity. The term $\frac{\mu}{\rho D}$ is also known as the Schmidt number ($\boldsymbol{S_c}$).

Turbulence model: The *k-epsilon* (*k-ε*) model is one of the most commonly implemented two-equation turbulence models in *CFD* to simulate mean flow characteristics for turbulent flow conditions. It represents the turbulent properties of the flow by means of two transport equations (*PDEs*). This allows accounting for history effects like convection and diffusion of turbulent energy. The *k-ε* model was developed to improve the mixing-length model, as well as to find an alternative to algebraically prescribing turbulent length scales in moderate to complex flows. with relatively small pressure gradients. The first transported variable is turbulent kinetic energy ($\boldsymbol{k}$) which determines the energy in the turbulence. The second one is the turbulent dissipation ($\boldsymbol{\varepsilon}$) and it determines the scale of the turbulence. The turbulence kinetic energy per unit mass $\boldsymbol{k}$ is defined as the variance of the fluctuations in velocity and has

dimensions of (*Length*) ^{2} * (*Time*) $^{-2}$. The turbulence eddy dissipation rate ε is the rate at which the velocity fluctuations dissipate and has dimensions of k per unit time – (*Length*) ^{2} * (*Time*) $^{-3}$. The *k-ε* model adds two new variables into the system of equations. The continuity equation and the momentum equation become *Eq. 16* and *Eq. 17*, respectively:

$$\frac{\partial \rho}{\partial t}+\frac{\partial}{\partial x_j}\left(\rho U_j\right)=0 \tag{16}$$

$$\frac{\partial \rho U_i}{\partial t}+\frac{\partial}{\partial x_j}\left(\rho U_i U_j\right)=-\frac{\partial p'}{\partial x_i}+\frac{\partial}{\partial x_j}\left[\mu_{eff}\left(\frac{\partial U_i}{\partial x_j}+\frac{\partial U_j}{\partial x_i}\right)\right]+S_M \tag{17}$$

Here, S_M is the sum of body forces, μ_{eff} is the effective viscosity accounting for turbulence, and p' is the modified pressure calculated using *Eq. 18:*

$$p'=p+\frac{2}{3}\rho k+\frac{2}{3}\mu_{eff}\frac{\partial U_k}{\partial x_k} \tag{18}$$

The term $\frac{2}{3}\mu_{eff}\frac{\partial U_k}{\partial x_k}$ involves the divergence of velocity and is neglected in *ANSYS CFX*. The model is based on the *eddy viscosity concept*, so that the effective viscosity is the sum of the molecular (dynamic) viscosity μ and the turbulence viscosity μ_t, as given in *Eq. 19*:

$$\mu_{\text{eff}}=\mu+\mu_{\text{t}} \tag{19}$$

It is assumed that μ_t is linked to the turbulence kinetic energy k and turbulence dissipation ε through the following *Eq. 20*, in which C_μ is a constant:

$$\mu_{\text{t}}=C_\mu \rho \frac{k^2}{\varepsilon} \tag{20}$$

The differential transport equations for the turbulence kinetic energy and the turbulence dissipation rate give the values for k and ε *(Eq. 21 and 22, respectively)*:

$$\frac{\partial(\rho k)}{\partial t}+\frac{\partial}{\partial x_j}\left(\rho U_j k\right)=\frac{\partial}{\partial x_j}\left[\left(\mu+\frac{\mu_t}{\sigma_k}\right)\frac{\partial k}{\partial x_j}\right]+P_k-\rho\varepsilon+P_{kb} \tag{21}$$

$$\frac{\partial(\rho\varepsilon)}{\partial t}+\frac{\partial}{\partial x_j}\left(\rho U_j \varepsilon\right)=\frac{\partial}{\partial x_j}\left[\left(\mu+\frac{\mu_t}{\sigma_\varepsilon}\right)\frac{\partial \varepsilon}{\partial x_j}\right]+\frac{\varepsilon}{k}\left(C_{\varepsilon 1}P_k-C_{\varepsilon 2}\rho\varepsilon+C_{\varepsilon 1}P_{\varepsilon b}\right) \tag{22}$$

Here, $C_{\varepsilon 1}$, $C_{\varepsilon 2}$, σ_ε and σ_k are constants and their values for this model are: $C_{\varepsilon 1}$=1.44, $C_{\varepsilon 2}$=1.92, σ_ε=1.3 and σ_k=1. P_{kb} and $P_{\varepsilon b}$ represent the influence of buoyancy forces, P_k is the turbulence production due to viscous forces and the way it is computated is given in *Eq. 23*:

$$P_k=\mu_t\left(\frac{\partial U_i}{\partial x_j}+\frac{\partial U_j}{\partial x_i}\right)\frac{\partial U_i}{\partial x_j}-\frac{2}{3}\frac{\partial U_k}{\partial x_k}\left(3\mu_t\frac{\partial U_k}{\partial x_k}+\rho k\right) \tag{23}$$

In our case, the full buoyancy model is used, so the buoyancy turbulence production term P_{kb} is modelled using *Eq. 24*:

$$P_{kb}=-\frac{\mu_t}{\rho\sigma_\rho}g_i\frac{\partial \rho}{\partial x_i} \tag{24}$$

Where σ_ρ is turbulent Schmidt number and is equal to 1 for the full buoyancy model. $P_{\varepsilon b}$ is considered to be proportional to P_{kb} (*Eq. 25*):

$$P_{\varepsilon b}=C_3\cdot\max\left(0,P_{kb}\right) \tag{25}$$

C_3 is a dissipation coefficient and in this case it is also equal to 1.

4. Results and Discussion

The main criterion for convergence of the solution is that the *RMS* (root-mean-square) value of the error in all elements is less than 10^{-6}. As convergence is too slow in some cases and the chosen *RMS* value may be reached after a long time, a secondary condition was defined – the maximum number of iterations is set to *1000*. When either of these two conditions is fulfilled, the solution stops. Two separate particle track objects were created – one that displays all generated tracks and one that isolates only the particle tracks, which reach the laser beam boundary (*Fig. 3*). The latter bears information regarding the diameter distribution and number flow rate of droplets which enter the laser beam volume.

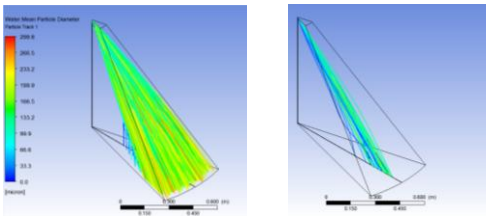

Fig. 3. *All droplet trajectories (left), and only the isolated trajectories, which cross the laser, beam (right).*

The number flow rate of droplets was calculated by taking the sum of the flow rates on each trajectory. This was done using the expression: *Sum (Water.Particle Number Rate) @ Particle Track.* The expression is evaluated once for the total flow rate of droplets generated by the nozzle and a second time to determine the flow rate of droplets through the laser beam. It should be noted again, that the calculated value of the number flow rate through the nozzle must be doubled to obtain the value of all droplets through the beam.

5. Conclusion

We have presented a numerical model for assessing fog parameters and have described the main mathematical algorithms that govern its execution.

Acknowledgements

This work has been funded by FP7-SEC-2012-1 program of the EU Commission under grant number 312804 and supported by the Bulgarian Ministry of Education and Science under the National Research Programme "Young scientists and postdoctoral students" approved by DCM # 577 / 17.08.

References

[1] Klassen S., The Photoelectric Effect: Reconstructing the Story for the Physics Classroom, *Science & Education*, 20(7):719-731, doi: 10.1007/s11191-009-9214-6

[2] Ivanov, O. Sensor applications of field-matter interactions. In *Encyclopedia of Sensors 9*; Grimes, C.A.; Dickey, E.I.; Pishko, M.V.; Eds.; American Scientific Publishers, Stevenson Ranch, California, USA, 2006; pp. 165-197, ISBN: 9781588830562.

[3] Ivanov O., Kuneva M., Quality control methods based on electromagnetic field-matter interactions, In *Application and Experience of Quality Control*, O. Ivanov (editor), INTECH, Vienna, 509-536 (2011) DOI: 10.5772/15857

[4] Park N. C., Abbate A., Das P., Characterization of Semiconductors by Laser-Generated Photocharge Voltage Spectroscopy, in *22nd International Symposium on Compound Semiconductors - Technologies*, Volume: 145, Cheju Island, Korea, 1996, pp. 593-598

[5] Perez-Diaz J. L., Qin Y., Ivanov O., Quinones J., Stengl V., Nylander K., Hornig W., Álvarez J., Ruiz-Navas E. M., Manzanec K., Fast Response CBRN High-Scale Decontamination System: COUNTERFOG: Science as the first countermeasure for CBRNE and Cyber threats, in book *Enhancing CBRNE Safety & Security: Proceedings of the SICC 2017 Conference*, Springer, 2018, 61-69, doi: 10.1007/978-3-319-91791-7_8

[6] Ivanov O., Karatodorov S., Pérez Díaz J.L.,. Novel Electromagnetic Sensor for Contaminations in Fog Based on the Laser-induced Charge Effect, *Proceedings of IEEE SENSORS 2017*, CFP17SE, IEEE, 2017, ISBN:978-1-5386-4056-2, 1509-1511

[7] Angelov K., Ivanov O., Todorov P., Pérez-Díaz J. L., Computational fluid dynamic model for estimating droplet number flow rate through a laser beam, *Security & Future*, 2, 2017, ISSN:2535-0668, 79-82